Enhancing X-Ray Generation by Electron-Beam–Laser Interaction in an Optical Bragg Structure

Vadim Karagodsky, David Schieber, and Levi Schächter
Department of Electrical Engineering, Technion—Israel Institute of Technology, Haifa 32000, Israel
(Received 16 April 2008; published 12 January 2010)

We demonstrate that x-ray radiation emitted by relativistic electrons scattered by a counter-propagating laser pulse guided by an adequate Bragg structure surpasses by about 2 orders of magnitude the energy generated by a conventional free-space Gaussian-beam configuration, given the same e beam and injected laser power in both configurations.

DOI: 10.1103/PhysRevLett.104.024801 PACS numbers: 41.60.−m, 52.38.Ph, 52.59.Px, 61.80.Fe

X-ray sources based on Compton scattering of a laser from a relativistic counterpropagating electron beam have been recently drawing increasing interest due to several potential advantages over undulators and wigglers [1], among which are compact size, significantly lower operation cost, and reduced e-beam energy requirement (tens MeV vs GeV). In recent years, several groups have reported successful x-ray generation relying on Compton scattering. In 2000, at the Brookhaven National Laboratory Accelerator Test Facility (BNL ATF) collaborators reported [2] generation of 6.5 keV photons by scattering a 60 MeV e beam from a 10.6 μm CO_2 laser. A collaboration at the Lawrence Livermore National Laboratory, at the PLEIADES facility, demonstrated generation of 78 keV x-ray photons [3] using a 57 MeV e beam and a 820 nm Ti:sapphire laser. An all-optical setup was reported more recently [4], employing a 800 nm Ti:sapphire laser split into two pulses: one used for the acceleration of electrons (5 MeV) and the second, counterpropagating pulse, used for Compton scattering. The emerging photons were measured to be in the range of 0.4 to 2 keV.

In order to ensure maximum field along the interaction region, in all Compton x-ray experiments, the *free-space* laser beam is focused to the size of the e beam cross section—see Fig. 1. Consequently, optical focusing of the laser limits the interaction region to about twice the Rayleigh length, being typically on the order of 1 mm [2,3] implying a relatively broad spectrum. Thus, any design is a compromise between two conflicting requirements: on the one hand a strong focusing is accompanied by strong field, facilitating high intensity x ray but a relatively broad spectrum; on the other hand, weak focusing leads to weak emission yet to a relatively sharp spectrum, as the interaction region is relatively long.

In this Letter we demonstrate that it is possible to avoid these conflicting requirements by replacing the free-space focused laser system with a configuration that employs a Bragg structure to *guide* the laser pulse [5–7]. Illustrated in Fig. 2, a Bragg waveguide consists of a subwavelength vacuum core, where the interacting electrons move, a matching layer [5] and a series of Bragg layers both ensuring tight radiation confinement—facilitating an electric field in excess of $1[\mathrm{GV/m}]$ [6]. For the same laser power as in free-space, the predicted x-ray intensity is by at least 1 order of magnitude higher and an important by-product is a significantly narrower spectrum. Furthermore, the Bragg waveguide can be designed to support a TEM mode within the vacuum core [5], which is important for keeping the maximal emission on axis as well as a higher degree of spatial uniformity which in turn reflects in a sharper spectrum. A different Bragg design was shown to be suitable for optical acceleration, by facilitating a TM_{01} mode within the vacuum core [6]. Relying on these two designs, the overall proposed setup is presented in Fig. 3. The all-optical process consists of two stages: first, the e beam is accelerated in an optical Bragg accelerating structure using a copropagating TM_{01} laser, after which the Compton scattering process takes place in a second Bragg waveguide, supporting a TEM laser propagating antiparallel to the e beam.

Having described the basic configuration, it is important to emphasize several details. In order to be able to consistently compare the proposed Bragg waveguide setup with a

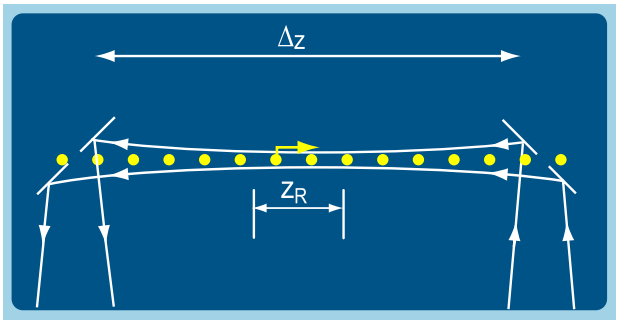

FIG. 1 (color online). Conventional Compton scattering setup. The laser is focused to a cross section of tens of microns. The interaction is limited by the Rayleigh length (z_R), which is typically at the order of 1 mm. The interaction between the e beam and the focused laser results in the emission of x ray, which forms a narrow cone having an opening angle of $1/\gamma$.

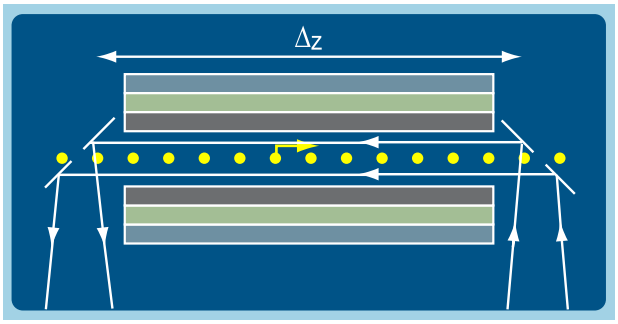

FIG. 2 (color online). Bragg waveguide setup. The electrons interact with a counterpropagating laser and emit x-ray radiation. The laser mode of interest has a TEM form inside the vacuum core. The mode is confined to a submicron cross section, enabling strong interaction not at the expense of interaction length.

conventional focused laser source, we assume both configurations to be driven by an identical e beam, both the laser power and laser linear polarization to be alike, and the interaction length, Δ_z (see Figs. 1 and 2), to be the same in both cases. It is the spatial variation of the wave amplitude (E_0) along the two interaction regions which differs. In what follows, the $\hat{z}$ axis indicates the direction of the e-beam trajectory, and the $\hat{x}$ axis indicates the polarization of the laser.

While in the Bragg configuration, taking the amplitude of the laser field to be uniform in the interaction region and zero otherwise is an excellent approximation, in the case of a focused Gaussian beam the amplitude of the field, as experienced by the electron, varies significantly. Nevertheless, in the framework of the analytic model whose assumptions are described next, we have found excellent agreement between the case employing the *exact* distribution of the amplitude and the case when an effective uniform amplitude (rms) is adopted—at least from the perspective of the overall emitted energy. The simplifying assumptions our analytic model relies upon are (i) a linearly polarized TEM mode, (ii) a weak interaction, (iii) head-on incidence, (iv) a relativistic e beam, and (v) uncorrelated emissions of the different electrons. Subject to these assumptions, the spectral density and the energy per unit solid angle are given by Eqs. (1)–(3).

$$\frac{d^2W}{d\omega d\Omega} \simeq \frac{dW}{d\Omega}\frac{N_{\mathrm{opt}}}{\omega_c(\theta,\gamma)}\mathrm{sinc}^2\left[\pi N_{\mathrm{opt}}\frac{\omega-\omega_c(\theta,\gamma)}{\omega_c(\theta,\gamma)}\right], \quad (1)$$

$$\frac{dW}{d\Omega} \simeq \kappa^2 N_{\mathrm{opt}}\alpha_F\hbar\omega_c(\theta,\gamma)\gamma^2\frac{[1-(\gamma\theta)^2]^2+4(\gamma\theta)^2\sin^2\phi}{[1+(\gamma\theta)^2]^4}, \quad (2)$$

$$\omega_c(\theta,\gamma) \simeq \omega_L\frac{4\gamma^2}{1+(\gamma\theta)^2}. \quad (3)$$

In these expressions $N_{\mathrm{opt}} = 2\Delta_z/\lambda_L$ is the number of optical laser periods experienced by an electron along the interaction length Δ_z, $\alpha_F \approx 1/137$ is the fine structure constant, $\omega_L = 2\pi c/\lambda_L$ is the laser angular frequency, θ and ϕ are the angular coordinates of the detector, θ being measured from the $\hat{z}$ axis, $\kappa = eE_0/m_0c\omega_L$ is the deflection parameter (also referred to as K factor), corresponding to the electromagnetic wiggler (laser), wherein E_0 is the *effective* amplitude experienced by the electron in the interaction region, m_0 and e are the electron rest mass and its elementary charge, respectively, and c is the speed of light in vacuum.

By virtue of linearity of Maxwell's equations, and by averaging over one laser period, the amplitude of the TEM mode supported by the Bragg waveguide is given by

$$E_0^2 = \frac{2\eta_0}{D_{\mathrm{int}}}\chi\left(\frac{P}{\Delta_y}\right); \quad (4)$$

$\eta_0 \equiv \sqrt{\mu_0/\epsilon_0}$ being the wave impedance in vacuum, P/Δ_y the injected average laser power per unit length (Δ_y), D_{int} the width of the internal vacuum core and except if other-

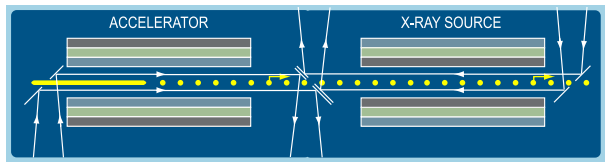

FIG. 3 (color online). Schematic of an all-Bragg system. In the left section the Bragg structure supports a TM_{01} mode which bunches and accelerates an electron beam. The latter is injected into another Bragg structure which supports a TEM mode (inside the vacuum core) which propagates antiparallel to the electrons that as a result generate x-ray radiation.

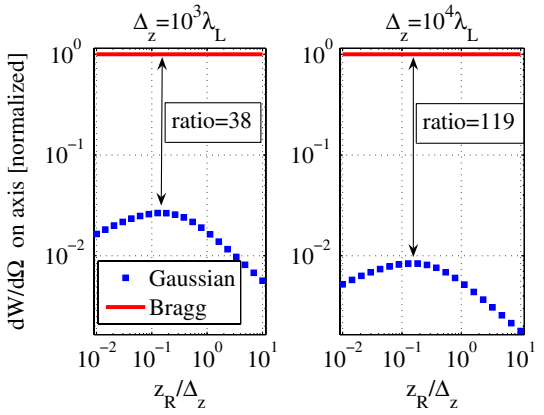

FIG. 4 (color online). Emitted energy per unit solid angle measured on the $\hat{z}$ axis in both setups. The normalization factor (same for all curves in each subfigure) is: $4N_{\mathrm{opt}}\alpha_F\kappa^2\hbar\omega_L\gamma^4$, wherein $\gamma = 50$ and $\kappa = eE_0/(mc\omega_L)$, E_0 being the E-field amplitude in Bragg waveguide configuration. The same e beam, laser power, interaction length ($\Delta_z = 10^3\lambda_L$, left and $\Delta_z = 10^4\lambda_L$, right) and polarization were assumed in both configurations.

wise specified, throughout this Letter it is assumed that $D_{\rm int} = 0.2\lambda_L$; χ is a *confinement factor* of the Bragg waveguide, representing the fraction of the laser power confined to the vacuum core relative to the total laser power in the waveguide. In the examples that follow we consider a conservative value of $\chi = 0.5$. Regarding a two-dimensional, linearly polarized and focused Gaussian beam, the effective amplitude E_0 is determined by the rms value that, on axis, can be approximated by

$$E_0^2 = \frac{4\eta_0}{\sqrt{2z_R\lambda_L}} \frac{\operatorname{arcsinh}(\frac{\Delta_z}{2z_R})}{\frac{\Delta_z}{2z_R}} \left(\frac{P}{\Delta_y}\right), \tag{5}$$

z_R being the Rayleigh length. For simplicity sake, in (5) it was tacitly assumed that the electrons are located on axis, where the Gaussian is maximal, providing an overestimate of the energy emitted in the case of a focused beam.

Based on these expressions [Eqs. (4) and (5)] for E_0, we are now in position to compare the emitted energy per solid angle ($dW/d\Omega$) in both configurations. For $\Delta_z = 10^3\lambda_L$, the left frame in Fig. 4 reveals that the intensity of the radiation emitted in the Bragg configuration is higher by at least 1 order of magnitude comparing to a focused beam configuration. An even clearer manifestation of this enhancement is revealed when examining a longer interaction length $\Delta_z = 10^4\lambda_L$ (right frame) in which case the intensity is higher by more than 2 orders of magnitude. These two frames reveal the essence of the concept presented in this study, namely, the inherent ability of a Bragg structure to confine most of the laser power in the vacuum core which is of subwavelength dimension.

In order to have some feeling as of the typical values involved, we refer to Table I where we calculate various quantities for electron energies varying from 5 to 250 MeV. Accordingly, the number of emitted photons per electron is independent of the kinetic energy $N_{\rm ph}/N_e = (2\pi/3)N_{\rm opt}\alpha_F\kappa^2 \simeq 2.8 \times 10^{-6}$. It is also interesting to note that the ratio between the two (Bragg and Gaussian) has an extremum at $z_R = 0.15\Delta_z$ given by Eq. (6).

$$\left[\frac{(dW/d\Omega)_{\rm Bragg}}{(dW/d\Omega)_{\rm Gauss}}\right]_{\rm min} = \frac{\chi\sqrt{\lambda_L\Delta_z}}{2.1D_{\rm int}}. \tag{6}$$

Figure 4 also illustrates quantitatively the compromise associated with the focusing process: on the one hand, in case of tight focusing ($z_R/\Delta_z < 0.1$), the angular spectrum ($dW/d\Omega$) is of low intensity associated with a short effective interaction length. On the other hand, for an extended effective interaction length ($z_R/\Delta_z > 1$), the emitted intensity is modest since the laser field is weak. Obviously these conflicting trends do not exist in the case of a Bragg waveguide setup and even for a conservative design ($\chi = 0.5$), the emitted energy exceeds by about 2 orders of magnitude the peak value in case of a free-space configuration.

TABLE I. Typical values of the emitted photons and of the linewidth (FWHM) for $E_0 = 1$ GV/m, $\lambda_L \simeq 1$ μm; $\Delta_z = 10^3\lambda_L$; $\kappa = eE_0/mc\omega_L \simeq 3 \times 10^{-4}$. The number of emitted x-ray photons per electron is in the order of $(2\pi/3)N_{\rm opt}\alpha_F\kappa^2 \simeq 2.8 \times 10^{-6}$.

Electron energy [MeV]	5	10	25	250
Peak energy of emitted photons [keV]	0.5	1.9	11.9	1192
Linewidth [eV]	0.2	0.8	5.3	528

Before concluding, let us make a few more comments: (i) Enhanced intensity as manifested in the analysis above has a direct effect on the achievable brightness. In Table II the results of two, state of the art, inverse Compton scattering experiments, are compared with our theoretical predictions for the spectral brightness attainable by our scheme. A reasonable formulation for the brightness, assuming $\kappa < 0.1$, is [10]:

$$B\left[\frac{\text{photons/ sec}}{\text{mm}^2 \times \text{mrad}^2 \times 0.1\%\text{BW}}\right] = \bar{B}J\left[\frac{\text{mA}}{\mu\text{m}^2}\right]\eta_{\theta_x}\eta_{\theta_y}. \tag{7}$$

$\bar{B}$ in (7) is the normalized brightness per unit e-beam current density, given by $\bar{B} = 4.55 \times 10^{10}(\kappa\gamma N_{\rm opt})^2$. In our model, we estimate $\bar{B}$ using the following parameters: $\kappa = 3.1 \times 10^{-4}$, $\gamma = 50$ and $N_{\rm opt} = 2 \times 10^4$ (in case of a 1 cm long device); the e-beam current density in (7) is denoted by J. Assuming that the e-beam cross section has a Gaussian shape with rms radii σ_x and σ_y, the current density is given by $J = \frac{I[\text{mA}]}{2\pi\sigma_x[\mu\text{m}]\sigma_y[\mu\text{m}]}$, I being the e-beam current. In many Compton scattering experiments, including those in Table II, the e beam bunch charge is of the order of nC, and the bunch length is of the order of psec. The typical e-beam cross section at the focal point is of the order of 0.01 mm^2. These parameters lead to a current density estimate of the order of $J = 100[\frac{\text{mA}}{\mu\text{m}^2}]$. It is reasonable to estimate that our structure can maintain similar current density as demonstrated in other Compton scattering experiments, with the sole difference that in our case the e-beam cross section will be highly elliptical (a ''sheet'' beam), as required by the narrow geometry of the vacuum core. η_{θ_i} in (7), where $i \in \{x, y\}$, is the efficiency coefficient, which describes degradation as a result of e-beam angular spread. It is given by $\eta_{\theta_i} = [1 + N_{\rm opt}(\gamma\delta\theta_i)^2]^{-1/2}$, $\delta\theta_i$ being the e-beam angular spread along the i axis. Using a purely geometrical argument for the scheme proposed in this study, it becomes evident that the angular spread $\delta\theta_x$, required for the e beam to pass through the narrow vacuum core without hitting the walls, is very small: $\delta\theta_x < D_{\rm int}/\Delta_z \ll (\gamma\sqrt{N_{\rm opt}})^{-1}$, resulting in $\eta_{\theta x}$ close to 1. We assume for simplicity that $\eta_{\theta y}$ is comparable to $\eta_{\theta x}$. Subject to the assumption specified above the brightness is of the order of $B = 4 \times 10^{17}[\frac{\text{photons/ sec}}{\text{mm}^2\times\text{mrad}^2\times 0.1\%\text{BW}}]$. This estimate is comparable to the experimental results in Table II, but it is achievable

TABLE II. Results of two recent state of the art inverse Compton scattering experiments.

	Peak spectral brightness $[\frac{\text{photons/sec}}{\text{mm}^2\times\text{mrad}^2\times 0.1\%\text{BW}}]$	Emitted photon energy	Electron energy	Laser wavelength [nm]
KEK + BNL [8]	1.7×10^{18}	56 [MeV]	1.28 [GeV]	532
LLNL [9]	10^{17}	65 [KeV]	56 [MeV]	815

with a laser power at least 2 orders of magnitude smaller due to intensity enhancement in the proposed paradigm. (ii) In a Bragg waveguide, extending the interaction region does not compromise the intensity of the laser. Therefore, narrow emission spectra are feasible. While a narrow spectrum is a desired quality for many applications, its implication is an enhanced sensitivity to e-beam parameters, in particular, to energy spread: $\delta\gamma/\gamma \lesssim 1/2N_{\text{opt}}$. (iii) It is assumed that the electrons can be injected and guided into the planar Bragg structure without causing wall damage. This assumption imposes a very stringent constraint on their angular spread (emittance) since based on pure geometric arguments, the electrons' angular spread should be at the most D_{int}/Δ_z. Consequently, the latter does not pose a serious difficulty on the emerging spectrum and more importantly, in order to obtain such a spread it is obvious that the electrons should be accelerated by a laser field in a Bragg acceleration structure of similar dimensions as the x-ray Compton structure discussed above. (iv) Although we have theoretically demonstrated significant improvement in efficiency over conventional setups for small K factors, it is important to highlight one limitation of this paradigm: at values of κ larger than 8×10^{-4} the use of the Bragg waveguide, becomes problematic due to nonlinear effects and surface damage caused by the laser pulse [6]. A free-space configuration (focused Gaussian beam) has virtually no limitation as it operates in vacuum reaching K factors of the order of unity [4,11,12]. However, we believe that this limitation is overshadowed by the inherent advantage of a Bragg structure associated with the small size of both the Bragg structure itself as well as that of the driving laser and accelerator—Fig. 3.

In conclusion, we have shown that in the weak Compton regime ($\kappa \ll 1$) the energy emitted by electrons when scattered by a counterpropagating laser pulse guided by a Bragg structure [5,6] surpasses by about 2 orders of magnitude the energy generated by a conventional free-space Gaussian-beam configuration, given the same e beam and injected laser power in both configurations. The enhanced radiation stems from the ability of a Bragg waveguide to confine a significant fraction of the power into a subwavelength region for an extended interaction length. While the sensitivity of the spectrum to electrons' energy spread is significant, the stringent constraint on the angular spread associated with the electron propagation in the vacuum tunnel of the Bragg-based structure, virtually eliminates the impact of the angular spread on the spectrum.

This study was supported by the Israel Science Foundation and the Kidron Foundation.

[1] H. Ōnuki and P. Elleaume, *Undulators, Wigglers, and their Applications* (CRC Press, Boca Raton, 2003).
[2] I. V. Pogorelsky *et al.*, Phys. Rev. ST Accel. Beams **3**, 090702 (2000).
[3] D. J. Gibson *et al.*, Phys. Plasmas **11**, 2857 (2004).
[4] H. Schwoerer *et al.*, Phys. Rev. Lett. **96**, 014802 (2006).
[5] A. Mizrahi and L. Schächter, Opt. Express **12**, 3156 (2004).
[6] A. Mizrahi and L. Schächter, Phys. Rev. E **70**, 016505 (2004).
[7] V. Karagodsky, A. Mizrahi, and L. Schächter, Phys. Rev. ST Accel. Beams **9**, 051301 (2006).
[8] I. Sakai *et al.*, Phys. Rev. ST Accel. Beams **6**, 091001 (2003).
[9] F. V. Hartemann *et al.*, *Proceedings of EPAC 2004* p. 270 (2004).
[10] D. Attwood, *Soft X-Rays and Extreme Ultraviolet Radiation: Principles and Applications* (Cambridge University Press, Cambridge, England, 2007).
[11] M. Babzien *et al.*, Phys. Rev. Lett. **96**, 054802 (2006).
[12] K. Ta Phuoc *et al.*, Phys. Rev. Lett. **91**, 195001 (2003).